Lack of *Schnurri-2* Expression Associates with Reduced Bone Remodeling and Osteopenia*

Yoshitomo Saita[‡], **Tsuyoshi Takagi**[§], **Keiichiro Kitahara**[‡], **Michihiko Usui**[‡], **Kohei Miyazono**[¶], **Yoichi Ezura**[‡||], **Kazuhisa Nakashima**[‡**1], **Hisashi Kurosawa**[‡‡], **Shunsuke Ishii**[§2], and **Masaki Noda**[‡||**§§3]

From the ‡Department of Molecular Pharmacology, Medical Research Institute, Tokyo Medical and Dental University, Tokyo 101-0062, §Laboratory of Molecular Genetics, RIKEN Tsukuba Institute, Ibaraki 305-0074, ¶Department of Molecular Pathology, Graduate School of Medicine, University of Tokyo, Tokyo 113-0033, ‡‡Department of Orthopedics, Juntendo University, School of Medicine, Tokyo 113-8421, and **21st Century Center of Excellence (COE) Program for the Frontier Research on Molecular Destruction and Reconstruction of Tooth and Bone, ||Advanced Bone and Joint Science Integrated Action Initiative in JSPS Core to Core Program, and §§Hard Tissue Genome Research Center, Tokyo Medical and Dental University, Tokyo 101-0062, Japan

Regulation of bone remodeling determines the levels of bone mass and its imbalance causes major skeletal diseases such as osteoporosis. A zinc finger protein, Schnurri-2 (SHN-2), was recently demonstrated to regulate bone morphogenetic protein-dependent adipogenesis and lymphogenesis. However, the role of SHN-2 in bone is not known. Here, we investigated the effects of *Shn-2* deficiency on bone metabolism and cell function in *Shn-2*-null mice. Lack of SHN-2 expression reduced bone remodeling by suppressing both osteoblastic bone formation and osteoclastic bone resorption activities *in vivo*. *Shn-2* deficiency suppressed osterix and osteocalcin expression as well as *in vitro* mineralization. Conversely, *Shn-2* overexpression enhanced osteocalcin promoter activity and bone morphogenetic protein-dependent osteoblastic differentiation. *Shn-2* deficiency suppressed *Nfatc1* and c-*fos* expression leading to reduction of tartrate-resistant acid phosphatase-positive cell development *in vivo* as well as in the cultures of bone marrow cells. These studies demonstrate that SHN-2 regulates the activities of critical transcription factors required for normal bone remodeling.

Adult bone is remodeled to meet continuously changing structural and metabolic requirements. To maintain bone mass, resorption by osteoclasts must be balanced by the formation of bone by osteoblasts. In bone diseases such as osteoporosis the balance between formation and resorption is lost, leading to reduced bone mass, which increases the risk of fractures (1, 2).

Identification of molecules involved in adult bone mass determination is critical to better understand the function of such molecules and may render clues for treatment of bone diseases such as osteoporosis. Several molecules have been reported to modulate adult bone mass in mouse models. Genetic analyses of high bone mass trait in the C3H strain and Balb strain identified a mutation in ALOX15 that may be responsible for increase in adult bone mass (3). Activating transcription factor 4 positively determines adult bone mass (4). Deficiency of transducer of erbB2 (TOB) and cas-interacting zinc finger protein (CIZ/NMP4) results in an increase in adult bone mass (5, 6). Loss of half the Runt-related transcription factor-2 (*Runx2*)[4] gene dosage causes failure in the recovery of trabecular bone mass after bone marrow ablation specifically in aged adult mice (7). In human, suppression of Wnt inhibitor signaling molecules such as Dickkopf increases adult bone mass (8), and loss of function mutation in sclerostin enhances adult bone volume in patients with sclerostosis (9). These molecules mostly act on osteoblasts to modulate only one of the two arms of bone remodeling.

Drosophila Schnurri (*Shn*) and mammalian *Shn* homologues *Shn-1*, *Shn-2*, and *Shn-3* are zinc finger-type molecules implicated in cell regulation of these species (10–19). SHN-2 was recently identified to regulate adipogenesis and lymphogenesis (20–22). SHN-2 binds to Smad proteins to up-regulate peroxisome proliferator-activated receptor γ gene expression (20), and it is also required for positive selection of thymocytes (21). SHN-2 competitively inhibits NF-κB binding and leads to the suppression of type 2 helper T cell differentiation (22). Recently, SHN-3, another member of the Schnurri family, was

1 To whom correspondence may be addressed: Dept. of Molecular Pharmacology, Medical Research Institute, Tokyo Medical and Dental University, 3-10 Kanda-Surugadai, 2-chome, Chiyoda-ku, Tokyo 101, Japan. Tel.: 81-3-5280-8067; Fax: 81-3-5280-8067; E-mail: kxn.mph@mri.tmd.ac.jp.
2 To whom correspondence may be addressed: Laboratory of Molecular Genetics, RIKEN Tsukuba Institute, 3-1-1 Koyadai, Tsukuba, Ibaraki 305-0074, Japan. Tel.: 81-29-836-9031; Fax: 81-29-836-9030; E-mail: sishii@rtc.riken.go.jp.
3 To whom correspondence may be addressed. Tel.: 81-3-5280-8066; Fax: 81-3-5280-8066; E-mail: noda.mph@mri.tmd.ac.jp.

4 The abbreviations used are: Runx2, Runt-related transcription factor-2; Shn, Schnurri; NFAT, nuclear factor of activated T cell; BMD, bone mineral density; BMP, bone morphogenetic protein; ALP, alkaline phosphatase; BFR, bone formation rate; M-CSF, macrophage colony-stimulating factor; RANKL, receptor activator of NF-κB ligand; MS/BS, mineralizing surface/bone surface; OPG, osteoprotegerin; WT, wild type; CT, computed tomography.
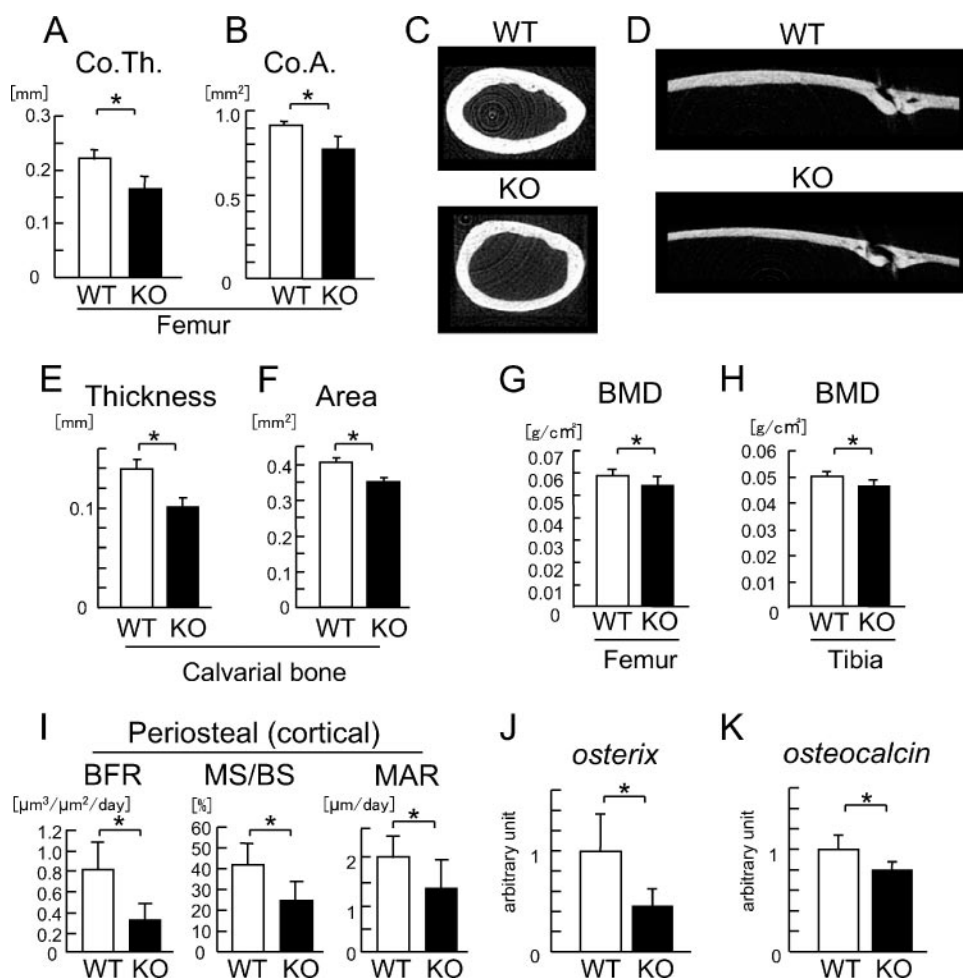
FIGURE 1. **Shn-2 deficiency suppressed bone mass and bone formation activity *in vivo*.** Cortical thickness (*Co.Th*) (*A*) and cortical area (*Co.A*) (*B*) levels in the midshaft of femur based on cross-sectional μCT analysis in wild type (*WT*) and *Shn-2*-deficient (*KO*) mice. *C*, cross-sectional two-dimensional μCT analysis of midshaft of femora. *D*, μCT analysis of parietal bone. *Shn-2* deficiency suppressed both thickness (*E*) and bone area (*F*) of parietal bone. *G* and *H*, bone mineral density (*BMD*) levels in femur (*G*) and tibia (*H*). *Shn-2* deficiency suppressed the levels of cortical bone volume as well as BMD. *I*, mineralized surface/bone surface (*MS/BS*), bone mineral apposition rate (*MAR*), and bone formation rate (*BFR*) were analyzed. *Shn-2* deficiency suppressed the levels of these dynamic bone formation parameters in cortical region. *J* and *K*, real-time reverse transcription PCR analysis of the levels of osterix (*J*) and osteocalcin (*K*) expression in bone. *Shn-2* deficiency suppressed the expression levels of these genes. These observations indicate that *Shn-2* deficiency-suppressed bone formation activity *in vivo* resulted in the loss of overall bone mass. *, $p < 0.05$.

mice and wild type littermates ($n = 7$) were used for the studies of bone mineral density (BMD), two-dimensional micro-computed tomography (μCT), bone histomorphometric analysis, bone marrow cell cultures, and measurement of BMP-induced alkaline phosphatase (ALP) activity. For experiments on the evaluations of time course study of two-dimensional micro-CT, we used 1-, 4-, and 8-week-old *Shn-2*-deficient mice and wild type littermates ($n = 3$). All the animal experiments were approved by the Animal Welfare Committee of Tokyo Medical and Dental University.

Measurement of BMD and μCT Analysis of Bone—BMD was measured based on dual-energy x-ray absorptiometry (DEXA) as described previously (24). Briefly, BMD (g/cm2) of the femora and tibia were subjected to dual x-ray absorptiometry using a device specifically designed for small animals (PIXI; GE Luner, Madison, WI). Two-dimensional μCT data were collected using the Musashi system (Nittetsu-ELEX, Osaka, Japan). For the evaluation of cortical bone volume, total cortical bone area as well as cortical thickness in the midshaft was measured. Calvarial thickness and bone area were measured in the coronal section of parietal bone. For cancellous bone, bone volume/tissue volume values were evaluated using μCT slices at the sagittal section of femora as well as coronal section of spine (L4) as described previously (24).

Histomorphometric Analysis and Skeletal Preparation—Bone formation rate (BFR) in cortical and cancellous regions in femora was measured in the undecalcified section as previously described (24). In the decalcified section, tartrate-resistant acid phosphatase-positive multinucleated cells were counted as osteoclasts to evaluate osteoclast number/bone surface and osteoclast surface/bone surface. Skeletal preparation was performed as described previously (25). Briefly, day 3 mice skins were removed and fixed in 95% EtOH overnight and then stained Alcian blue (15 mg/100 ml in 80% EtOH) followed by alizarin red (5 mg/100 ml in 2% KOH).

RNA Extraction, cDNA Synthesis, and PCR—RNA was extracted from mouse femur, MC3T3E1 cells, and RAW264.7 cells based on the acid guanidinium thiocyanate-phenol-chloroform method. First-strand cDNA was synthesized using 1 μg of the total RNA and Molony murine leukemia virus

reported to suppress adult bone mass levels through RUNX2 protein degradation (23). However, SHN-3 shares only limited homology with SHN-2 (17).

Here, we report on *Shn-2* deficiency-suppressed bone formation as well as bone resorption. *Shn-2* deficiency reduced the expression levels of osteoblastic transcription factor osterix as well as osteoclastic transcriptional factors, nuclear factor of activated T cells (*Nfat*) c1 and c-*fos*. *Shn-2* overexpression enhanced promoter activity of osteocalcin, which is downstream of master regulators in osteoblasts. Furthermore, *Shn-2* overexpression activated bone morphogenetic protein (BMP)-induced osteoblastic differentiation. Thus, *Shn-2* is a novel regulator of adult bone remodeling.

EXPERIMENTAL PROCEDURES

Animals—*Shn-2* knock-out mice were described previously (21). Male BALB/c background 12-week-old *Shn-2* knock-out
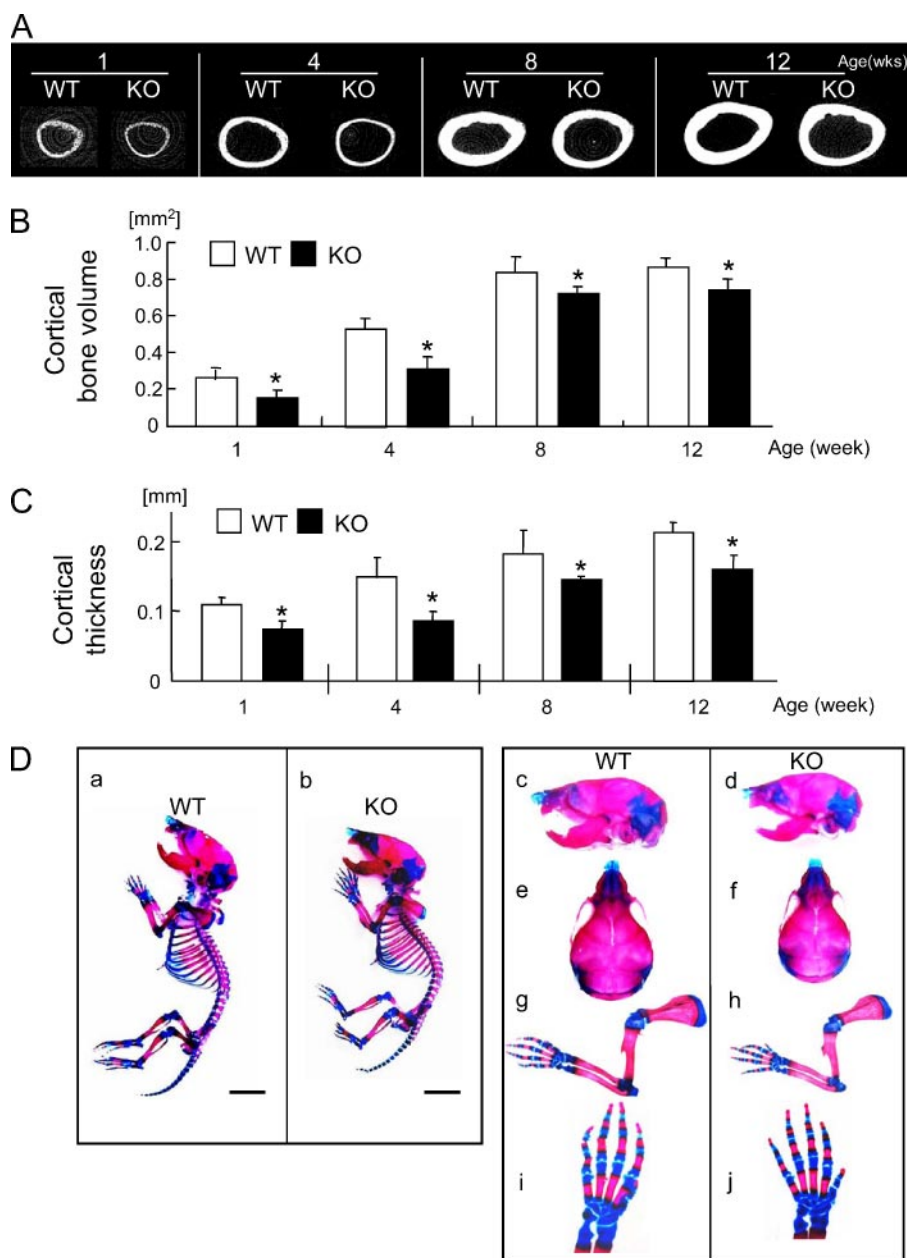
A

FIGURE 2. **Deficiency of *Shn-2* suppressed cortical bone volume at growing as well as adult stages.** *A*, cross-sectional two-dimensional micro-CT images of midshaft of the femora at indicated ages of WT and KO mice. Cortical bone volume (*B*) and cortical thickness (*C*) in these mice. *Shn-2* deficiency suppressed cortical bone mass as early as 1 week after birth up to at least the age of 12 weeks. *D*, alizarin red/Alcian blue staining of the skeleton of WT (*a*) and *Shn-2*-deficient (*KO*) (*b*) mice was performed at postnatal day 3. *Scale bar*, 5 mm. Close-ups of the skull of WT (*c*, *e*) and KO (*d*, *f*), forelimbs (*g*, *h*), and hands (*i*, *j*). *Shn-2*-deficient mice did not exhibit any abnormalities in skeletal patterning but were smaller in size.

CAG GTT AGG G-3′, reverse, 5′-TCG GTT TCT TAG GGT CTT GGA GTG-3′; osterix, forward, 5′-AGC GAC CAC TTG AGC AAA CAT C-3′, reverse 5′-CGG CTG ATT GGC TTC TTC TTC C-3′; *Alp*, forward, 5′-GCT ATC TGC CTT GCC TGT ATC TG-3′, reverse, 5′-AGG TGC TTT GGG AAT CTG TGC-3′; *Rankl*, forward, 5′-CCT GAG GCC CAG CCA TTT-3′, reverse, 5′-CTT GGC CCA GCC TCG AT-3′; osteoprotegerin (*Opg*), forward, 5′-TAC CTG GAG ATC GAA TTC TGC TT-3, reverse, 5′-CCA TCT GGA CAT TTT TTG CAA A-3′; c-*fos*, forward, 5′-CCG TGT CAG GAG GCA GAG C-3′, reverse 5′-GCA GCC ATC TTA TTC CGT TCC C-3′; *Nfatc1*, forward, 5′-AGC CCA AGT CTC ACC ACA GG-3′, reverse, 5′-CAG CCG TCC CAA TGA ACA GC-3′; and glyceraldehyde-3-phosphate dehydrogenase, forward, 5′-AGA AGG TGG TGA AGC AGG CAT C-3′, reverse, 5′-CGA AGG TGG AAG AGT GGG AGT TG-3′.

Cells—Primary osteoblasts were obtained from the outgrowth cultures of bone fragments of calvariae taken from wild type and *Shn-2*-deficient mice. These cells were used for measurement of BMP-induced ALP activity. Bone marrow cells were flushed out after the proximal epiphyseal ends were removed from right tibiae of wild type and *Shn-2*-deficient mice and used for mineralized nodule formation assay and osteoclast development. Osteoclastogenesis was examined both in bone marrow cells and splenocytes obtained from wild type and *Shn-2*-deficient mice. The MC3T3E1 osteoblastic cell line was obtained from RIKEN (Saitama, Japan). These cells were used for experiments of real-time PCR, overexpression of *Shn-2*, and luciferase assays. The RAW264.7 cell line was purchased from the Dainippon Pharmaceutical Co., Ltd. and maintained with Dulbecco's modified Eagle's medium containing 10% fetal bovine serum. These cells were used for experiment of RANKL (100 ng/ml)-induced *Shn-2* mRNA expression.

Bone Marrow Cultures—Marrow cells were plated in 24-well plates (2.0 cm²/well) at a density of 2×10^6 cells/well. Tartrate-resistant acid phosphatase-positive osteoclast-like multinucleated cells were formed in α-minimal essential medium supplemented

reverse transcriptase. Amplification was performed as described previously (26).

Quantitative real-time PCR was performed using iQ SYBR Green Supermix (Bio-Rad). The quantification was done as described previously (27). Expression values were normalized to glyceraldehyde-3-phosphate dehydrogenase. The primers for real-time reverse transcription PCR were as follows: *Shn-2*, forward, 5′-GCC GCC CAC CCT GAC TTA C-3′, reverse, 5′-CTT CTC ATC CAC ACT GCT CTT GC-3′; *Col1a1*, forward, 5′-CTG ACT GGA AGA GCG GAG AG-3′, reverse, 5′-GCA CAG ACG GCT GAG TAG G-3′; *Runx2*, forward, 5′-TGG CTT GGG TTT
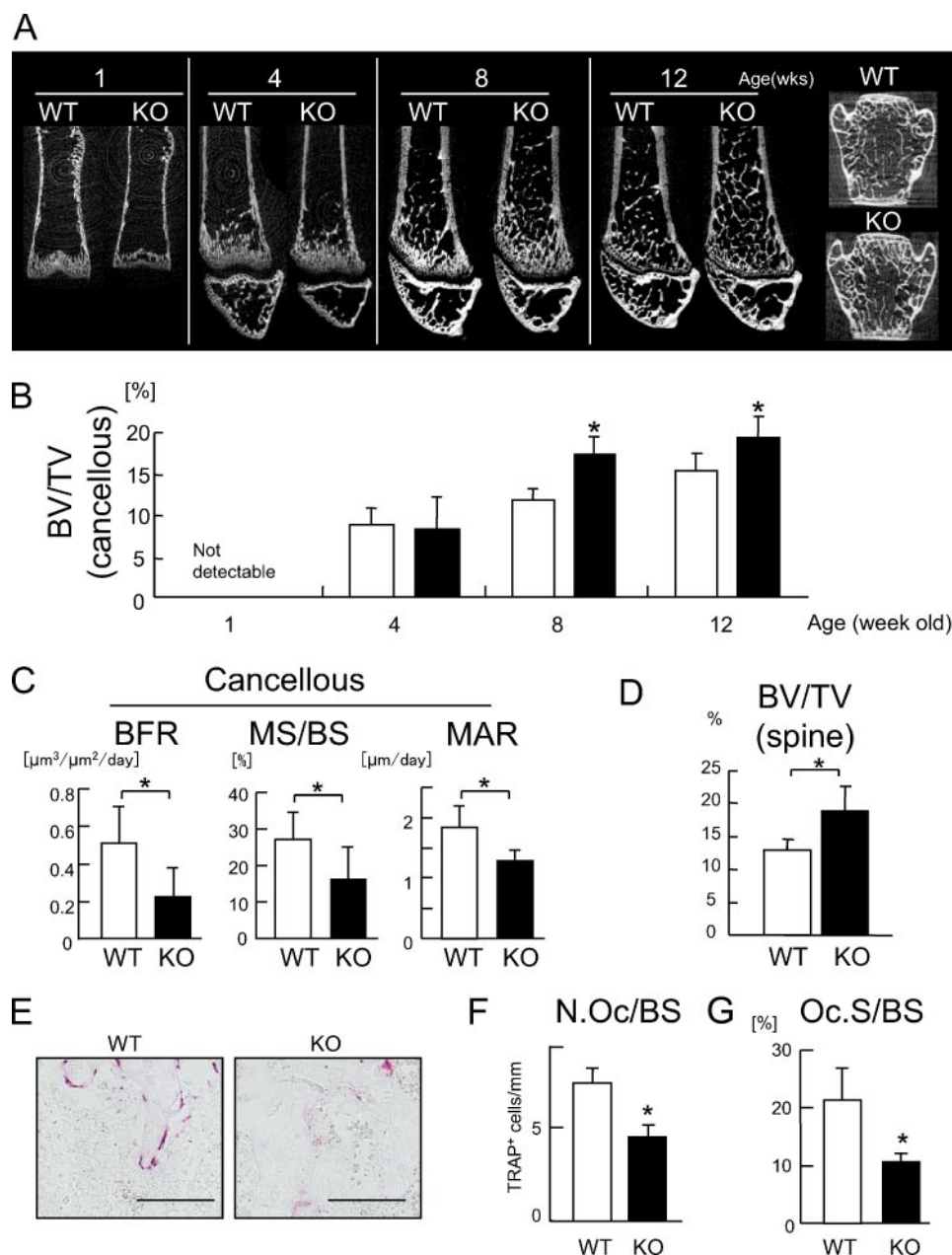
FIGURE 3. **Cancellous bone volume was increased in *Shn-2*-deficient mice after 8 weeks in association with suppression in bone resorption activity.** *A*, saggital section of two-dimensional micro-CT images of distal end of femora at indicated ages and coronal section of lumbar spine at 12 weeks old. *B*, time course analysis of bone volume/tissue volume of secondary trabecular bone in WT and KO mice. In 1-week-old mice, secondary trabecular bones were barely detectable in micro-CT analysis. Trabecular bone volume was higher in *Shn-2*-deficient mice than wild type after 8 weeks. *C*, *Shn-2* deficiency suppressed dynamic bone formation parameters similarly to the suppression seen in cortical bone (Fig. 1*I*). *D*, Trabecular bone volume of lumbar spine at 12 weeks old. *E*, tartrate-resistant acid phosphatas staining of the decalcified sections at the proximal ends of the tibiae in WT and KO mice. *Scale bar*, 100 μm. Osteoclast number/BS (*F*) and osteoclast surface/BS (*G*) were measured as described under "Experimental Procedures." *Shn-2* deficiency suppressed both osteoclast number/BS and osteoclast surface/BS levels.

face was measured by using the Luzex-F automated image analyzer (Nireco).

Measurement of ALP Activity— ALP activity measurement was made in primary osteoblasts by using *p*-nitrophenyl phosphate as substrate (28). These cells were maintained in α-minimal essential medium. Cell differentiation was induced by treatment with 100 ng/ml rhBMP-2 in a standard growth medium.

Transfections and Reporter Assays—MC3T3E1 cells (1×10^5 cells/well in six-well tissue culture plates) were transfected with various combinations of the following plasmids using the FuGENE 6 transfection reagent: reporter constructs (12×GCCG/luciferase, 1.1 kb osteocalcin-gene-2/luciferase), *Shn-2* expression vector, and empty vector as a control. After 24–72 h of incubation, cell extracts were prepared and used to measure luciferase activity based on the Dual Luciferase™ reporter assay system (Promega), and the values were normalized against the efficiency of transfection using the same system. Both firefly and *Renilla* luciferase activities were measured by AutoLumat (LB953; EG & G Brethhold).

Osteoclastogenesis in Stromal Cell-free Condition—Lymphocytes and monocytes were obtained from spleen by using Lympholite-M (Cedarlane) according to the manufacturer's protocol. These cells were cultured for 12 h with 5 ng/ml macrophage colony-stimulating factor (M-CSF), and non-adherent cells were further cultured in the presence of 30 ng/ml M-CSF for 3 days. RANKL (100 ng/ml) was added with 30 ng/ml M-CSF, and tartrate-resistant acid phosphatase-positive multinucleated cells were counted as osteoclasts.

with 10% fetal bovine serum, 100 μg/ml antibiotics-antimycotics mixture, 10 nM 1.25(OH)$_2$ vitamin D$_3$, and 100 nM dexamethasone. The medium was changed every 3–4 days. For mineralized nodule formation, bone marrow cells were cultured in a standard growth medium containing 50 μg/ml ascorbic acid and 10 mM sodium β-glycerophosphate. The medium was changed every 3–4 days. The cultures were stained in a saturated solution of alizarin red on day 21. The area of mineralized nodules/total dish surface

Statistical Evaluations—The results were presented as mean values ± S.D. Statistical analysis was performed by Student's *t* test to evaluate differences between the two groups. Analysis of variance was performed when the examined experimental groups exceeded three groups. Tukey's multiple comparison test was applied as post hoc test. *p* values <0.05 were considered to be statistically significant.
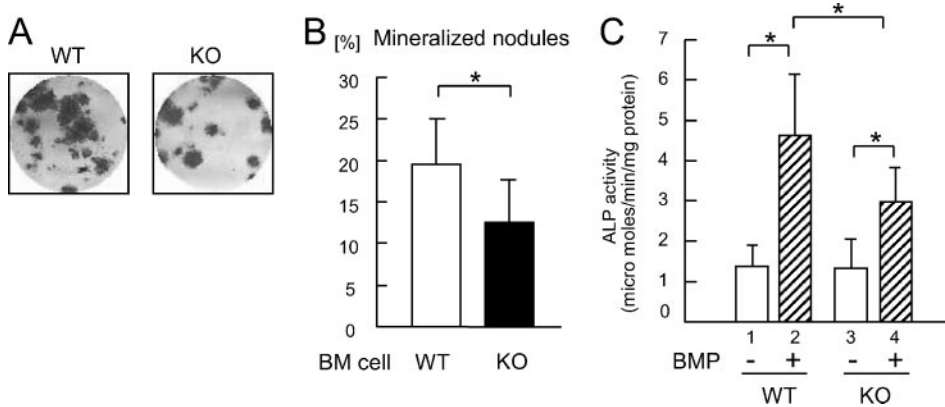
FIGURE 4. **Shn-2 deficiency suppressed osteoblastic differentiation.** *A* and *B*, *Shn-2* deficiency suppressed formation of mineralized nodules in bone marrow cells. *C*, alkaline phosphatase (*ALP*) activity was examined in calvaria-derived cells obtained from WT and KO mice in the presence or absence of rhBMP-2 (100 ng/ml) in culture. *Shn-2* deficiency suppressed osteoblastic differentiation in these cells.
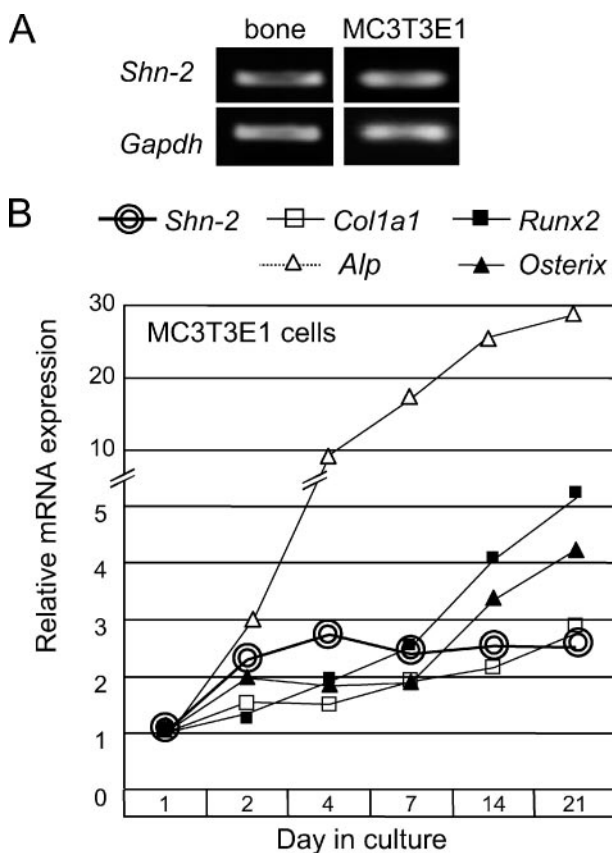

FIGURE 5. **Shn-2 expression in osteoblast-like cells *in vitro*.** *A*, *Shn-2* mRNA expression was detected in bone *in vivo* and in MC3T3E1 cells. *B*, MC3T3E1 cells were cultured for 21 days. RNA was extracted at the indicated time points. Expression levels of *Col1a1*, *Runx2*, osterix, *Alp*, and *Shn-2* were estimated based on real-time PCR system. Expression levels of genes related to osteoblastic phenotypes were gradually increased in these cells. Expression level of *Shn-2* was enhanced in these cells up to day 4 and kept at similar expression level up to day 21.

RESULTS

Cortical bone is the major component of adult bone mass. *Shn-2* deficiency reduced cortical bone mass with respect to the levels of cortical thickness and cortical bone area in femora (Fig. 1, *A–C*) and in calvarial bone (Fig. 1, *D* and *F*). Because the size and length of femur of *Shn-2*-deficient mice were smaller than

wild type (21), we also evaluated the values of cortical thickness and cortical area normalized against those of femur length and found that *Shn-2* deficiency reduced cortical bone parameters after normalization as well (data not shown). This observation was further supported by reduction in BMD in *Shn-2*-deficient mice (Fig. 1, *G* and *H*). Thus, *Shn-2* deficiency reduced total bone mass.

With respect to dynamic parameters, *Shn-2* deficiency suppressed the levels of BFR as well as mineral apposition rate (MAR) and mineralizing surface (MS/BS) in the periosteal regions of cortical bone (Fig. 1*I*). These observations indicated that SHN-2 is required for the activities of individual osteoblastic cells (mineral apposition rate) as well as the mineralizing surface (MS/BS) to maintain BFR. We also counted osteoblast number as defined by Parfitt *et al.* (29) because MS/BS represent osteoblast surface but do not represent the number of osteoblast. Although *Shn-2* deficiency tended to suppress the number of osteoblast, it was not statistically significant (data not shown). Molecular bases for such *Shn-2* deficiency phenotype in bone mass were further examined based on mRNA expression levels in whole bone *in vivo*. Messenger RNA expression levels of osteoblastic phenotype-related genes such as osterix and osteocalcin were suppressed in the bones of the *Shn-2*-deficient mice (Fig. 1, *J* and *K*). Expression of other maker genes, including *Col1a1*, *Runx2*, and *Alp*, tended to be decreased in *Shn-2*-deficient mice though they were not statistically significant. Therefore, *Shn-2* deficiency suppressed bone formation activity *in vivo* at the messenger RNA levels.

We examined the bones of mice at younger stages, including the time points of 1, 4, and 8 weeks after birth. Although overall contour of the cortical bone in the cross-section of the midshaft was similar (Fig. 2*A*), cortical bone volume (Fig. 2*B*) and cortical thickness (Fig. 2*C*) were less in *Shn-2*-deficient mice compared with wild type 1 week after birth; this reduction was similarly observed in 4-, 8-, and 12-week-old mice (Fig. 2, *A–C*). In younger mice such as 3 days old, examination of skeletal preparation did not reveal major defects (Fig. 2*D*). Thus, SHN-2 is required for the regulation of osteoblasts.

Although *Shn-2* deficiency resulted in overall reduction in the levels of parameters in bone mass as represented by the data in whole limb bone BMD (Fig. 1, *G* and *H*), there was a regionally and temporally limited mild increase in bone volume/tissue volume in the cancellous bone envelope in the metaphysis of *Shn-2*-deficient mice (Fig. 3*A*). This phenotype was limited to 8- and 12-week-old mice and was not observed in 4-week-old mice (Fig. 3, *A* and *B*). These data indicated that *Shn-2* deficiency reduced bone mass (including cortical and cancellous) after mice were 1 week old. However, they were associated with regional (limited to metaphyseal region) cancellous bone increase at the adult stage (8 and 12 weeks).
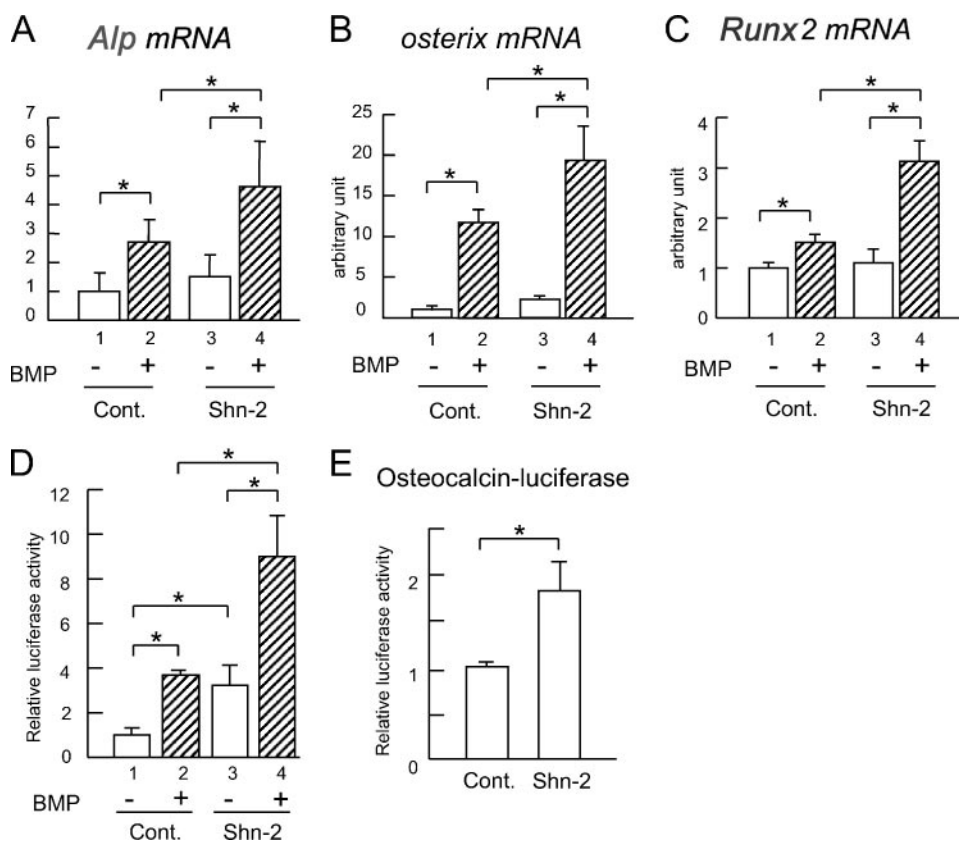
FIGURE 6. **Shn-2 overexpression enhanced osteoblastic differentiation.** MC3T3E1 cells were transfected with empty or *Shn-2* expression vector and expression levels of *Alp* (*A*), osterix (*B*), and *Runx2* (*C*) mRNA were measured after 48 h of incubation in the presence or absence of rhBMP-2. *D*, a luciferase reporter gene containing concatameric Smad1-dependent BMP response elements (12 × GCCG) and *Shn-2* expression vector were co-transfected into MC3T3E1 osteoblastic cells, which were subsequently exposed to rhBMP-2 (200 ng/ml) for 2 days. *E*, luciferase activity of 1.1 kb mouse osteocalcin gene in MC3T3E1 cells. *Shn-2* overexpression enhanced authentic promoter of mouse osteocalcin gene.

blastic cells using bone marrow cells of the wild type and *Shn-2*-deficient mice. *Shn-2* deficiency suppressed the levels of mineralized nodule formation in bone marrow cells cultured in the presence of β-glycerophosphate and ascorbic acid (Fig. 4, *A* and *B*). During the differentiation of osteoblasts in these bone marrow cell cultures, BMP signaling was reported to play a critical role (31, 32). Therefore, we examined SHN-2 involvement in BMP signaling. For those experiments, we prepared cells outgrown from the explants of minced calvarial bones. The basal levels of ALP in these wild type and *Shn-2*-deficient cells derived from the calvaria were similar (Fig. 4*C*, *lane 1 versus 3*). BMP-2 enhanced ALP activity ~3-fold in wild type cells, whereas *Shn-2* deficiency suppressed this BMP effect on ALP down to 2-fold (Fig. 4*C*, *lane 2 versus 4*; $p < 0.05$). To further examine *Shn-2* expression in osteoblastic cell line, we examined MC3T3E1 cells. *Shn-2* mRNA was expressed in osteoblastic MC3T3E1 cells (Fig. 5*A*). During the cultures of MC3T3E1 cells, *Shn-2* mRNA levels increased ~2.5-fold within 4 days in culture along with the increase in the expression levels of alkaline phosphatase (Fig. 5*B*, *Alp*). After day 4 in culture, *Shn-2* mRNA levels stayed at steadily high levels, whereas the mRNA levels of osteoblastic differentiation marker genes, such as *Alp*, *Runx2*, osterix, and type I collagen (*Col1a1*) gradually increased up to day 21 (Fig. 5*B*). Therefore, *Shn-2* expression levels were increased along with maturation of osteoblasts during the early differentiation stage.

Shn-2 overexpression in osteoblastic cell line MC3T3E1 promoted BMP-2 enhancement in the expression levels of *Alp*, osterix, and *Runx2* mRNAs (Fig. 6, *A–C*). These data revealed that SHN-2 is a positive regulator of osteoblastic differentiation, which acts at least in part by modulating BMP actions in these cells.

To examine the mode of SHN-2 modulation of BMP signaling, BMP-induced transcriptional events were studied. *Shn-2* overexpression by itself enhanced ~3-fold the expression of luciferase reporter gene linked to the BMP response elements, 12 × GCCG, in MC3T3E1 cells (Fig. 6*D*, *lane 1 versus 3*). This enhancement was similar to that observed in the cells receiving BMP treatment alone (Fig. 6*D*, *lane 2 versus 3*). Under this condition, *Shn-2* overexpression enhanced luciferase levels ~2-fold more than those observed in the BMP-induced transcriptional activation (Fig. 6*D*, *lane 2 versus 4*).

To further elucidate this point, in addition to cortical bone we conducted analyses on the dynamic bone formation parameters in cancellous bone envelope. The data revealed that *Shn-2* deficiency suppressed the levels of cancellous MS/BS, mineral apposition rate, and BFR (Fig. 3*C*), consistent with the observation on these parameters in cortical bone (Fig. 1*I*). Although *Shn-2* deficiency suppressed bone formation activities in cancellous bone, trabecular bone volume was increased in the metaphysis of long bone. To see whether this phenotype was restricted to long bone or not, we also evaluated trabecular bone volume in spine. Trabecular bone volume at the lumbar spine also increased in 12-week-old *Shn-2*-deficient mice compared with wild type (Fig. 3, *A* and *D*). Previously reported animal models, such as mice deficient in SHN-3, TOB, and CIZ, only revealed osteoblastic phenotype, but not osteoclastic phenotype (5, 23, 30). In contrast to these previous models, *Shn-2* mutation "suppressed" bone resorption parameters, including osteoclast number/BS and osteoclast surface/BS levels (Fig. 3, *E* and *G*). Thus, *Shn-2* deficiency has a unique feature in that it causes reduction in both osteoblastic and osteoclastic activities *in vivo* to lead to low turnover state in bone.

To better understand how SHN-2 acts in cells, we examined *Shn-2* expression in osteoblastic cells. We tested whether SHN-2 is functionally involved in the differentiation of osteo-

To see whether SHN-2 affects transcription of authentic promoter of gene encoding osteoblastic phenotype, a 1.1-kb osteo-
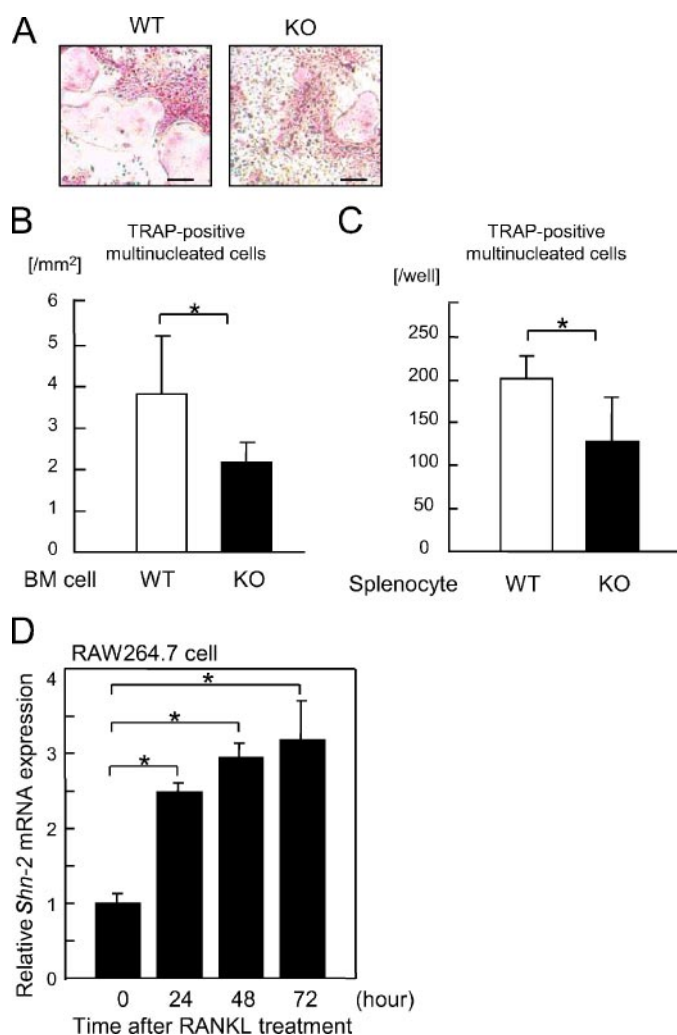
FIGURE 7. **Shn-2 deficiency suppressed osteoclastogenesis in culture.** *A* and *B*, osteoclast development in the culture of bone marrow cells obtained from WT and KO mice. *Shn-2*-deficient bone marrow cells exhibited impairment in tartrate-resistant acid phosphatase-positive cell development. *Scale bar,* 500 µm. *C*, osteoclastogenesis in stromal cell-free condition. Splenocytes were obtained from WT and KO littermates. Tartrate-resistant acid phosphatase-positive cells were induced by M-CSF and RANKL treatment as described under "Experimental Procedures." *Shn-2* deficiency significantly suppressed RANKL-dependent osteoclastogenesis. *D*, *Shn-2* expression in RAW264.7 cells with RANKL (100 ng/ml) treatment for indicated time points. *Shn-2* was expressed in RAW264.7 cells, and its expression was enhanced after RANKL stimulation.

calcin promoter construct was transfected into MC3T3E1 cells. Overexpression of *Shn-2* enhanced the activity of osteocalcin promoter (Fig. 6*E*). These observations indicate that SHN-2 enhances bone formation and osteoblastic differentiation at least in part through its action on transcriptional events that are involved in osteoblastic differentiation.

Shn-2-deficient mice exhibited *in vivo* osteoclastic phenotype in bone whereas *Shn-3*-deficient mice did not (23). We therefore pursued the mode of this SHN-2 action in osteoclastogenesis. Bone marrow cells were cultured in the presence of vitamin D$_3$ and dexamethasone. *Shn-2* deficiency suppressed the development of osteoclasts in the bone marrow cell culture (Fig. 7, *A* and *B*). As bone marrow cell cultures contain both stromal cells and progenitor cells for osteoclasts, we wished to test whether SHN-2 contributes to osteoclastogenesis in pro-

genitor cells. For this purpose, spleen cells, which contain osteoclast progenitors but less stromal cells, were subjected to osteoclastogenesis assay in cultures in the presence of M-CSF and soluble receptor activator of NF-κB ligand (RANKL). *Shn-2* deficiency in spleen cells reduced the development of osteoclasts in culture (Fig. 7*C*). These data revealed that SHN-2 acts as an endogenous modulator to support osteoclastogenesis. With regard to osteoclast function, *Shn-2*-deficient cells could form an actin ring and resorb dentin slice (data not shown), suggesting that absence of SHN-2 impaired in RANKL-dependent osteoclast development but not function. To examine *Shn-2* expression during osteoclastic cell differentiation, RAW264.7 cells were treated with RANKL. RAW264.7 cells differentiated into tartrate-resistant acid phosphatase-positive multinucleated cells in the presence of RANKL without M-CSF as reported previously (33). Therefore, the effects of RANKL alone could be observed in these cells. *Shn-2* mRNA expression levels in RAW264.7 cells were enhanced by RANKL treatment (Fig. 7*D*). Thus, *Shn-2* expression is under the control of RANKL signaling, and at the same time it is supporting osteoclast development.

Shn-2 deficiency suppressed the function of osteoblast, which is the main source of RANKL and OPG. Impaired osteoclastogenesis in *Shn-2* deficiency would be caused by the suppression of the induction of RANKL by osteoblasts. Thus, we analyzed expression levels of *Rankl* as well as *Opg* in bone. We found that *Rankl* expression levels were enhanced by *Shn-2* deficiency (Fig. 8*A*), whereas expression levels of *Opg* tended to decrease in *Shn-2* deficiency without statistical significance (Fig. 8*B*). *Rankl/Opg* ratio significantly increased in *Shn-2*-deficient mice (Fig. 8*C*). Therefore, impaired osteoclastogenesis in *Shn-2* deficiency occurred despite the elevated *Rankl*.

Because osteoclastogenesis is under the control of RANKL signaling, we analyzed expression levels of the genes downstream of this signaling. Expression level of *c-fos* was decreased in the bones of *Shn-2*-deficient mice (Fig. 8*D*). Because c-*fos*-deficient mice were reported to exhibit severe osteopetrosis due to impaired osteoclastogenesis (34) and c-*fos* targets NFATc1 (35, 36), we also examined the expression level of *Nfatc1*. Expression levels of *Nfatc1* were decreased in the bones of *Shn-2*-deficient mice (Fig. 8*E*). These results suggest that SHN-2 is involved in the RANKL-induced signals to promote osteoclast development. Although the interactions between RANKL and BMP on osteoclastogenesis remain unclear, BMP has been recently reported to positively regulate osteoclastic activities *in vivo* (37). Our preliminary data also indicated that BMP treatment enhanced RANKL-induced osteoclastogenesis in wild type spleen cells, whereas such BMP enhancement in osteoclastogenesis was suppressed in *Shn-2*-deficient cells.

DISCUSSION

We report here that SHN-2 is a novel transcriptional regulator of bone cell function and bone mass. *Shn-2* deficiency caused reduction in whole bone BMD *in vivo* and suppressed bone formation as well as bone resorption parameters. Thus, SHN-2 plays a role in both arms of bone metabolism involved in bone turnover and remodeling.
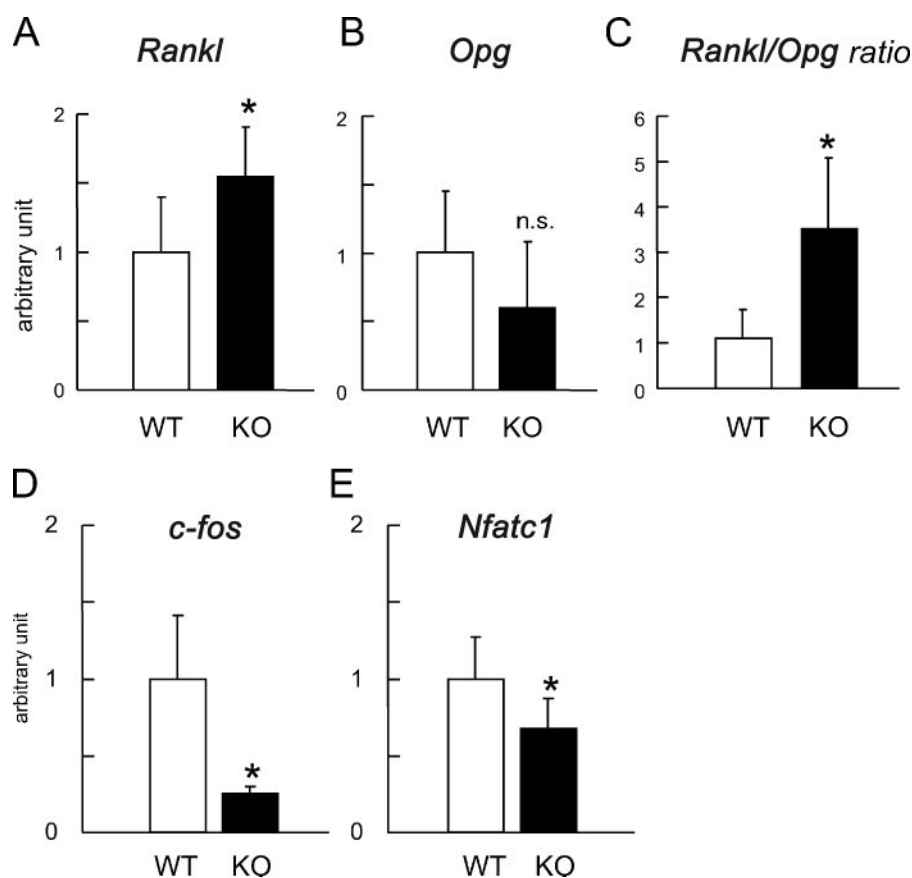
FIGURE 8. **Shn-2 deficiency suppressed expression levels of genes encoding critical transcription factors in osteoclastic cell lineage *in vivo*.** Real-time PCR analysis of *Rankl* (*A*), *Opg* (*B*), c-*fos* (*D*), and *Nfatc1* (*E*). RNA was taken from the bones of wild type and *Shn-2*-deficient mice. Real-time PCR was performed as described under "Experimental Procedures." The expression level of *Rankl* was increased while *Opg* was decreased in *Shn-2* deficiency, leading to high *Rankl/Opg* ratio (*C*). Deficiency of *Shn-2* suppressed the expression levels of c-*fos* as well as its target gene *Nfatc1 in vivo*, suggesting the involvement of *Shn-2* downstream of the RANKL-induced signals.

why *Shn-2* deficiency causes short stature remains unclear. In growth plate, the columnar structures and primary spongiosa appeared normal. As *Shn-2* deficiency slightly increased the length of growth plate, *Shn-2* deficiency may result in failure to remodel calcified cartilage.

As observed in *in vivo* analyses, one of the important points in SHN-2 actions is to regulate both osteoclastic and osteoblastic cells. Molecular analyses of osteoclastic activities indicated that deficiency of *Shn-2 per se* suppressed c-*fos* and *Nfatc1* expression levels *in vivo*. In the presence of RANKL, *Shn-2* enhanced the levels of osteoclastic differentiation in RAW264.7 cells and also the promoter activity of *Nfatc1* (data not shown). Therefore, in osteoclastic differentiation SHN-2 would again be a transcriptional modulator of the promoter of *Nfatc1*, possibly by working together with other transcriptional factors or modulators such as NFATc1 by itself.

Bone formation and bone resorption would be often regulated simultaneously in the same direction (2, 38, 39), called coupling. Such a coupling event is important for the body to maintain bone mass. For instance, enhancement of bone formation in the event of loss of bone due to the increase in bone resorption would benefit the maintenance of bone mass (39, 40). Although understanding the mechanisms of this coupling is important, molecular bases for these coupling phenomena have not yet been fully elucidated (34, 36, 41). Compensatory mechanisms would provide for repair of lost bone to resume bone mass level under physiological conditions. However, in the case of postmenopausal osteoporosis, enhancement in bone resorption exceeds that of bone formation to end up with eventual bone loss (1, 36). As SHN-2 acts positively in both bone formation and resorption, this molecule plays a role at least in part to support the coupling events during the remodeling cycle to maintain adult bone mass. Our preliminary experiments of co-culture assays using osteoblasts and spleen cells from wild type and *Shn-2*-deficient mice revealed that *Shn-2* deficiency in both osteoblasts and osteoclasts suppressed osteoclastogenesis (data not shown). This observation supported that SHN-2 plays a role in both osteoblasts and osteoclast to support osteoclastogenesis.

Shn-2 deficiency has been reported to suppress adipogenesis by reducing the BMP signaling in fat tissue (20) and lymphogenesis by suppressing conversion from the double positive thymocytes into single positive cells, respectively (21, 22). BMP has been recently reported to positively regulate osteoclastic

Shn-2 deficiency resulted in reduction in osterix and downstream osteocalcin gene expression. We also found that overexpression of *Shn-2* enhanced the levels of this gene. Thus, SHN-2 would be a modulator of at least one of the two master regulatory molecules of osteoblastic differentiation, osterix. Overexpression experiments indicated that SHN-2 by itself enhanced BMP response element-dependent transcription, possibly due to the enhancement of endogenous BMP. This SHN-2 action was observed to be augmented in the case of the simultaneous presence of exogenously added BMP. Furthermore, even in the absence of BMP, SHN-2 alone enhanced the osteocalcin gene in the 1.1-kb promoter, indicating that SHN-2 is acting on the gene either alone or in combination with the endogenous BMP signaling. We also observed that in the absence of SHN-2, suppression of osterix in bone was observed. However, *Runx2* suppression was not obvious, suggesting that SHN-2 may act to modulate the function of osteoblastic master regulatory molecules more at the stages of osterix action that is downstream to the RUNX2 action. As it is obvious that SHN-2 *per se* is dispensable for osteoblastic differentiation, the importance of SHN-2 activity is to modify the levels of differentiation in osteoblastic cell lineages.

Shn-2 deficiency decreased the length of long bone (data not shown) as well as the body weight (20, 21). However, the reason

activities *in vivo* (37) and also has been implicated in regulation of immune cells (42). Our observations on SHN-2 action in bone coincides with these notions on the close relationship between bone, fat, and immune system although a direct relationship among those still needs to be elucidated.

It is intriguing to note those mice deficient in *Shn-2* and those deficient in *Shn-3* exhibit opposite phenotypes, *i.e.* osteopenia *versus* osteosclerosis, respectively (23). In addition, *Shn-2*-deficient mice revealed osteoclastic phenotype whereas *Shn-3*-deficient mice did not. Although zinc finger motifs are present in both molecules, overall homology is relatively low (<30%) (17). These features suggest that the two molecules would not compensate each other but rather they would be required for distinct functions in the regulation of bone metabolism.

In conclusion, SHN-2 is a novel regulator of bone cells that plays a role in the maintenance of the bone mass, acting via positive regulation of transcription factors required for the functions of osteoblasts and osteoclasts.

REFERENCES

1. Raisz, L. G. (2005) *J. Clin. Investig.* **115,** 3318–3325
2. Martin, T. J., and Sims, N. A. (2005) *Trends Mol. Med.* **11,** 76–81
3. Klein, R. F., Allard, J., Avnur, Z., Nikolcheva, T., Rotstein, D., Carlos, A. S., Shea, M., Waters, R. V., Belknap, J. K., Peltz, G., and Orwoll, E. S. (2004) *Science* **303,** 229–232
4. Yang, X., Matsuda, K., Bialek, P., Jacquot, S., Masuoka, H. C., Schinke, T., Li, L., Brancorsini, S., Sassone-Corsi, P., Townes, T. M., Hanauer, A., and Karsenty, G. (2004) *Cell* **117,** 387–398
5. Yoshida, Y., Tanaka, S., Umemori, H., Minowa, O., Usui, M., Ikematsu, N., Hosoda, E., Imamura, T., Kuno, J., Yamashita, T., Miyazono, K., Noda, M., Noda, T., and Yamamoto, T. (2000) *Cell* **103,** 1085–1097
6. Shen, Z. J., Nakamoto, T., Tsuji, K., Nifuji, A., Miyazono, K., Komori, T., Hirai, H., and Noda, M. (2002) *J. Biol. Chem.* **277,** 29840–29846
7. Tsuji, K., Komori, T., and Noda, M. (2004) *J. Bone Miner. Res.* **19,** 1481–1489
8. Morvan, F., Boulukos, K., Clement-Lacroix, P., Roman, S., Suc-Royer, I., Vayssiere, B., Ammann, P., Martin, P., Pinho, S., Pognonec, P., Mollat, P., Niehrs, C., Baron, R., and Rawadi, G. (2006) *J. Bone Miner. Res.* **21,** 934–945
9. Gardner, J. C., van Bezooijen, R. L., Mervis, B., Hamdy, N. A., Lowik, C. W., Hamersma, H., Beighton, P., and Papapoulos, S. E. (2005) *J. Clin. Endocrinol. Metab.* **90,** 6392–6395
10. Grieder, N. C., Nellen, D., Burke, R., Basler, K., and Affolter, M. (1995) *Cell* **81,** 791–800
11. Arora, K., Dai, H., Kazuko, S. G., Jamal, J., O'Connor, M. B., Letsou, A., and Warrior, R. (1995) *Cell* **81,** 781–790
12. Staehling-Hampton, K., Laughon, A. S., and Hoffmann, F. M. (1995) *Development* **121,** 3393–3403
13. Udagawa, Y., Hanai, J., Tada, K., Grieder, N. C., Momoeda, M., Taketani, Y., Affolter, M., Kawabata, M., and Miyazono, K. (2000) *Genes Cells* **5,** 359–369
14. Marty, T., Muller, B., Basler, K., and Affolter, M. (2000) *Nat. Cell Biol.* **2,** 745–749
15. Dai, H., Hogan, C., Gopalakrishnan, B., Torres-Vazquez, J., Nguyen, M., Park, S., Raftery, L. A., Warrior, R., and Arora, K. (2000) *Dev. Biol.* **227,** 373–387
16. Affolter, M., Marty, T., Vigano, M. A., and Jazwinska, A. (2001) *EMBO J.* **20,** 3298–3305
17. Wu, L. C. (2002) *Gene Expr.* **10,** 137–152
18. Oukka, M., Wein, M. N., and Glimcher, L. H. (2004) *J. Exp. Med.* **199,** 15–24
19. Durr, U., Henningfeld, K. A., Hollemann, T., Knochel, W., and Pieler, T. (2004) *Eur. J. Biochem.* **271,** 1135–1144
20. Jin, W., Takagi, T., Kanesashi, S. N., Kurahashi, T., Nomura, T., Harada, J., and Ishii, S. (2006) *Dev. Cell* **10,** 461–471
21. Takagi, T., Harada, J., and Ishii, S. (2001) *Nat. Immunol.* **2,** 1048–1053
22. Kimura, M. Y., Hosokawa, H., Yamashita, M., Hasegawa, A., Iwamura, C., Watarai, H., Taniguchi, M., Takagi, T., Ishii, S., and Nakayama, T. (2005) *J. Exp. Med.* **201,** 397–408
23. Jones, D. C., Wein, M. N., Oukka, M., Hofstaetter, J. G., Glimcher, M. J., and Glimcher, L. H. (2006) *Science* **312,** 1223–1227
24. Kitahara, K., Ishijima, M., Rittling, S. R., Tsuji, K., Kurosawa, H., Nifuji, A., Denhardt, D. T., and Noda, M. (2003) *Endocrinology* **144,** 2132–2140
25. Hogan, B., Beddington, R., Costantini, F., and Lacy, E. (1994) *Manipulating the Mouse Embryo*, 2nd Ed., 379–381, Cold Spring Harbor Laboratory Press, Cold Spring Harbor, NY
26. Pfaffl, M. W. (2001) *Nucleic Acids Res.* **29,** 2002–2007
27. Salingcarnboriboon, R., Yoshitake, H., Tsuji, K., Obinata, M., Amagasa, T., Nifuji, A., and Noda, M. (2003) *Exp. Cell Res.* **287,** 289–300
28. Maeda, Y., Tsuji, K., Nifuji, A., and Noda, M. (2004) *J. Cell Biochem.* **93,** 337–344
29. Parfitt, A. M., Drezner, M. K., Glorieux, F. H., Kanis, J. A., Malluche, H., Meunier, P. J., Ott, S. M., and Recker, R. R., (1987) *J. Bone Miner. Res.* **2,** 595–610
30. Morinobu, M., Nakamoto, T., Hino, K., Tsuji, K., Shen, Z. J., Nakashima, K., Nifuji, A., Yamamoto, H., Hirai, H., and Noda, M. (2005). *J. Exp. Med.* **201,** 961–970
31. Lecanda, F., Avioli, L. V., and Cheng, S. L. (1997) *J. Cell Biochem.* **67,** 386–396
32. Takeuchi, Y., Watanabe, S., Ishii, G., Takeda, S., Nakayama, K., Fukumoto, S., Kaneta, Y., Inoue, D., Matsumoto, T., Harigaya, K., and Fujita, T. (2002) *J. Biol. Chem.* **277,** 49011–49018
33. Hirotani, H., Tuohy, N. A., Woo, J. T., Stern, P. H., and Clipstone, N. A. (2004) *J. Biol. Chem.* **279,** 13984–13992
34. Grigoriadis, A. E., Wang, Z. Q., Cecchini, M. G., Hofstetter, W., Felix, R., Fleisch, H. A., and Wagner, E. F. (1994) *Science* **266,** 443–448
35. Boyle, W. J., Simonet, W. S., and Lacey, D. L. (2003) *Nature* **423,** 337–342
36. Zelzer, E., and Olsen, B. R. (2003) *Nature* **423,** 343–348
37. Okamoto, M., Murai, J., Yoshikawa, H., and Tsumaki, N. (2006) *J. Bone Miner. Res.* **21,** 1022–1033
38. Harada, S., and Rodan, G. A. (2003) *Nature* **423,** 349–355
39. Winslow, M. M., Pan, M., Starbuck, M., Gallo, E. M., Deng, L., Karsenty, G., and Crabtree, G. R. (2006) *Dev. Cell* **10,** 771–782
40. Felsenberg, D., and Boonen, S. (2005) *Clin. Ther.* **27,** 1–11
41. Epstein, S. (2005) *Mayo Clin. Proc.* **80,** 379–388
42. Bleul, C. C., and Boehm, T. (2005) *J. Immunol.* **175,** 5213–5221